Available online at www.sciencedirect.com

ScienceDirect

Procedia CIRP 45 (2016) 335 – 338

www.elsevier.com/locate/procedia

3rd CIRP Conference on Surface Integrity (CIRP CSI)

Quantitative x-ray analysis: applications in machining of porous metallic foams

H. Qiao, S. Basu, C. Saldana*

G. W. Woodruff School of Mechanical Engineering, Georgia Institute of Technology, Atlanta, GA 30308 USA

* Corresponding author. Tel.: +1-404-385-3735; fax: +1-404-894-9342. *E-mail address:* christopher.saldana@me.gatech.edu

Abstract

In the present study, surface integrity in the face milling of open-cell aluminum metal foams was studied at full-volume using micro-computed tomography. Morphological damage to the pore-strut network of the foam was characterized as a function of machining parameters. Post-mortem surface integrity characteristics including effective pore size, foam porosity, and depth of the deformation-affected zone were characterized using the voxel-based data. The machined surface exhibits spatially-graded characteristics, featuring distinct regions of foam-strut bending/buckling and fracture. Implications of these observations for understanding effects on performance relative to structural bio-medical applications and integrity optimization strategies are described.

Peer-review under responsibility of the scientific committee of the 3rd CIRP Conference on Surface Integrity (CIRP CSI)

Keywords: Machining; Metal Foams; Computed Tomography; Surface Integrity

1. Introduction

Cellular solids can be found in a range of structural applications in naturally-occurring biological systems and, somewhat more recently, in engineered applications. A host of characteristics of biological open volume materials in terms of cellular architecture, shape, size and topology gives rise to unique thermal, electrical, acoustic and mechanical properties [1, 2]. Their utility in engineering applications has been seen, for example, in the biomedical sector where porous metal solids are promising for addressing issues related to stress shielding and biointegration in hard implants [3]. Porous metals are produced by a number of methods ranging from specialized casting routes to additive metal deposition. Although net shape processing of porous metals by additive manufacturing may reduce the overall number of processing steps, volume production is limited to billet-form processing wherein machining is required to achieve final implant geometry.

To leverage the potential for engineered cellular structures to optimize properties (e.g., weight, stiffness, strength, biointegration), advances in their end-to-end manufacture, including final shaping, are strongly needed. While porous metal foams are important toward improving performance in terms of lightweighting and bsiointegration, fundamental deformation and failure mechanisms and the mechanics of processing of hard foams are not well understood. In comparison, significant attention has been paid to investigate mechanics of damage and failure of foams in generalized loading platforms, including tension and compression using 3D non-destructive imaging [4-7]. Unfortunately, material response in primary manufacturing processes used to bring porous foams to final form (e.g., machining, forming) has mostly received empirical treatment [8-15].

Thermomechanical loading in machining of open cell foams is substantially more complex than in uniaxial loading due to the heterogeneity present within the foam network. This deformation heterogeneity gives rise to localized damage (e.g., smearing, fracture) in the machined surface and structural damage throughout the subsurface in terms of changes to the pore and strut network [8-15]. The heterogeneous foam structural characteristics are critical factors to consider for these novel materials due to their direct effects on functional performance. For biological foams, it is well known that damage to cell morphology disrupts the interconnected foam network, limiting biointegration and reducing implant integrity [3, 16].

In this regard, full-volume measurements of surface damage in machined foams are critical toward understanding corresponding effects on performance. To address this need, the present study seeks to investigate surface integrity of machined metal foams using full-volume characterization by computed tomography, whereby tomographic imaging is used to assess changes to the pore and strut network as a function of processing parameters.

Peer-review under responsibility of the scientific committee of the 3rd CIRP Conference on Surface Integrity (CIRP CSI)
doi:10.1016/j.procir.2016.03.019

Table 1. Experimental conditions.

Condition	Depth of Cut (*mm*)	Cutting Speed (*m/s*)	Feed (*mm/tooth*)
A	2	2.6	0.051
B	2	2.6	0.102
C	2	5.2	0.051

2. Experimental Details

The milling operation of the open cell metal foams was performed using a two-flute, 50 mm face mill with uncoated carbide inserts. The work materials were open-cell aluminum 6061-T6 foams obtained in rectangular blocks with dimensions of 90 mm * 40 mm * 13 mm, as shown in Figure 1. The machining center, a TRAK K3 EMX Mill, was used to machine the specimen surface in a single machining pass at a cutting speed of 2.6 and 5.2 m/s, a feed rate of 0.051 and 0.101 mm/min/tooth rate and a cutting depth of 2 mm, as shown in Table 1. Herein, milling parameters were advised from prior investigations of process induced damage on metal foams. In this regard, it is also anticipated that a large depth of cut would suitably amplify damage induced and aid in delineation of the underlying process physics. Structural characterization of the initial and post-machined foam samples was carried out using a micro-computed tomography platform (Zeiss Metrotom), with an effective spatial resolution of 57 μm/voxel. The X-ray tube of the tomographic platform was used under scanning conditions of 50 kV and 70 μA, corresponding to a 5 μm focal spot size. During the tomographic scan, the original and deformed foam samples were rotated in incremental steps over a total angular range of 360 degrees to facilitate three-dimensional image acquisition.

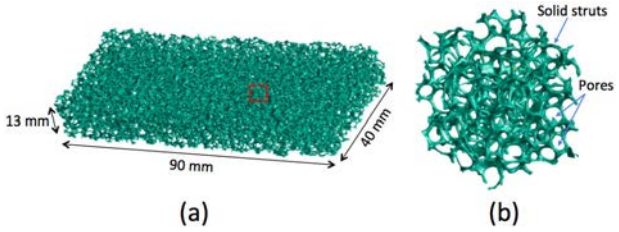

Fig. 1. (a) Initial foam structure and (b) elements of foam structure, including solid struts and connected pores.

The X-ray beam transmitted through the sample was collected on a planar detector with a sensor size of 1,536 px * 1,900 px. The set of resulting projections taken over different angular increments was processed using cone-beam reconstruction to yield individual image slices of the three-dimensional solid, wherein each image slice corresponded to unit voxel thickness. The stack of digital slices was then imported into MATLAB to reconstruct three-dimensional foam structure, shown in Figure 1. To facilitate further image processing and because of high contrast from distinct X-ray interaction between air and solid phases, a global grey level threshold was applied to facilitate binary transformation of the three-dimensional images identifying different solid/air regions. For measurement of pore morphology and effective pore size, a MATLAB-based watershed analysis code was developed [17, 18]. The analysis code assigned each pore in the low density solid a unique label based on the concept of a three-dimensional distance map wherein each voxel center has a value of distance to the nearest solid-phase voxel and each pore centroid is located at relative peaks in the distance map. To facilitate direct comparisons between the initial and post-machined samples a volumetric registration algorithm was also developed to align the data sets based on inherent structural markers in the open cell foams.

3. Results

The effects of machining on the surface structure of the foam samples was observed in structural changes to both solid strut configurations and the resulting pore morphology. Figure 2 shows voxel models for both the initial and the post-machined foam samples for condition A (e.g., V_c = 2.6 m/s, f = 0.051 mm/tooth) obtained at a depth of d = 3 mm from the machined surface, as well as the resulting pore mapping using the MATLAB-based tomographic analysis. From the figure, it is clear that the machining of the foam resulted in noticeable differences in the solid strut network due to strut fracture and local strut rotations. The resulting effects on pore morphology are also noticeable in terms of changes to pore aspect ratio and relative diameter.

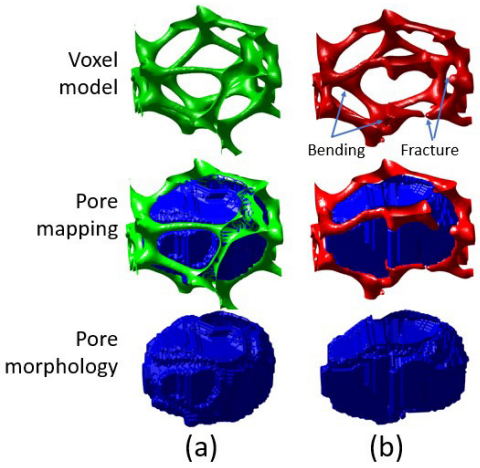

Fig. 2. Analysis of individual pore geometries for (a) undeformed and (b) deformed metallic foams with original voxel models, watershed analysis results and pore morphology. Foam shown is for condition A in Table 1. Green: pristine, Red: deformed, Blue: Void geometry

The effects of the machining process on average pore size and relative porosity were mapped as a function of depth from the machined surface using the quantitative computed tomographic analyses. Figure 3(a)-(c) shows the evolution of equivalent pore diameter as a function of subsurface depth for the experimental conditions investigated. For condition A (e.g., V_c = 2.6 m/s, f = 0.051 mm/tooth), the initial undeformed aluminum foam had an effective pore diameter in range of 1.75 mm to 2.25 mm. After machining, the near-surface structure unto a subsurface depth of 4.11 mm was clearly altered by the material removal process while the extents of the workpiece remained un-